EAI Endorsed Transactions
on Pervasive Health and Technology
Research Article EAI.EU

Hybrid glaucoma detection model based on reflection components separation from retinal fundus images

Satyabrata Lenka[1], Zefree Lazarus Mayaluri[2,*]

[1,2]Department of Electrical Engineering, C. V. Raman Global University, Bhubaneswar, Odisha, India

Abstract

The diagnosis of diseases associated to the retina is significantly aided by retinal fundus images. However, when flash illumination is used during image acquisition, specularity reflection can occur on images. The retinal image processing applications are popular now days in diseases detection such as glaucoma, diabetic retinopathy, and cataract. Many modern disease detection algorithms suffer from performance accuracy limitation due to the creation of specularity reflection problem. This research proposes a preprocessing step for specularity removal from corrupted fundus images using a modified dichromatic reflection model. We develope a hybrid model for screening of glaucoma which includes a preprocessing step to separate specular reflections from corrupted fundus images, a segmentation step using modified U-Net CNN, a feature extraction step, and an image classification step using support vector machine (SVM) with different kernels. Firstly, the diffuse and specular components are obtained using seven existing methods and apply a filter having high emphasis with a function called similar in each component. The best method, which provides highest quality images, is chosen among the seven compared methods and the output image is used in next steps for screening of glaucoma. The experimental results of the proposed model show that in preprocessing step, maximum improvement in terms of PSNR and SSIM are 37.97 dB and 0.961 respectively. For glaucoma detection experiment the results have the accuracy, sensitivity, and specificity of 91.83%, 96.39%, and 95.37% respectively and AUROC of 0.971.

Keywords: Fundus image, Glaucoma, Specularity, Diffusion, CNN

Received on 30 March 2023; accepted on 28 May 2023; published on 10 July 2023

doi:10.4108/eetpht.9.3191

1. Introduction

In recent years, retinal imaging has become a common tool in the medical diagnosis of visual illnesses as glaucoma, cataract, and diabetic retinopathy [1]. Fundus cameras are frequently used to obtain retinal images, which depict the internal anatomies such as the optic disc, retinal vessels, and optic cup. By conducting a thorough investigation of these retinal images, it is confirmed that the changes found in these retinal structures are symptomatic of a pathological condition connected to diseases like glaucoma and diabetic retinopathy. Retinal image analysis is thus a practical and beneficial diagnostic technique. In reality, by determining the root cause of the issue, analysis of retinal images can be helpful in classifying the stages of eye diseases. So, the image processing approaches mainly depends on the quality of the images, which further depends on the illumination level of the light sources.

Whenever light enters into the eye and passes through a transparent protective layer called the cornea, much light are specularly reflected due to the curvature surface of eye. The light then falls onto the retina which senses the visual signals by passing through the pupil and lens. As there is no internal light in the eye, an external source provides light at the time of image capturing. The retinal fundus

*Corresponding author. Email: zefree.lazarus@cgu-odisha.ac.in

images captured by fundus cameras mainly suffer from non-uniform illumination, low contrast, and blurriness. These problems are arises by the presence of other diseases such as cataract, and unusual movement of eye with a degree of dilation. The non-uniform illumination in the fundus imaging mainly creates shadows and specular reflections [2]. As the automatic detection of retinal diseases by using fundus images depends upon the important features present in the fundus images such as optical cupping, the quality of the retinal images need to be high. This study is focused on enhancement of the quality of retinal fundus images by separating the specular reflection problem for efficient glaucoma detection. Figure 1 shows a sample of fundus images from the online available datasets with OD, OC, and ISNT area and visual fields with normal and glaucomatous eye.

Glaucoma an eye disease causes peripheral vision loss and gradually leading to blindness. The unbalancing of drainage of aqueous humour causes an increase in Intra Ocular Pressure (IOP) inside the eye, due to which the optic nerves connected from human eye to brain get damage. An efficient vision mainly depends upon the health condition of optic nerves as it sends visual messages to the brain [3]. Glaucoma cannot be cured, only early detection can prohibit its progression. The ophthalmologists conduct periodical check up and comprehensive eye examination such as regular vision test, slit lamp test, IOP measurement, and perimetry test to diagnose glaucoma. However these tests require regular check-up with appropriate instrumentation, experienced ophthalmologist, more time, and high cost.

A brief study of OD and OC in fundus images plays a vital role for glaucoma detection. The increase in disc and cup area is measured to calculate a most important clinical indicator for glaucoma called cup to disc ratio (CDR). Large CDR value shows more risk of glaucoma while smaller CDR value indicates healthy eye condition. ISNT rule is also another important indicator for diagnosis of glaucoma [4]. The important features such as disc area, cup area, blood vessels, and Neuroretinal rim are extracted and used for classification of images as glaucoma or non-glaucoma.

The automatic diagnostic approaches for glaucoma using Machine Learning (ML) and Deep Learning (ML) fully depend on extracted features from retinal fundus images. For extracting important features, the specular reflection problem in the fundus images should be eliminated. According to Shafer's dichromatic model [5] of image formation, every material produces two types of reflections particularly diffuse and specular reflections. As the fundus images also have specularity problem due to non-uniform illumination in the fundus imaging, our aim is to separate the specular component from the original corrupted image as a preprocessing step and further the diffused component will be used in the next steps for accurate glaucoma detection.

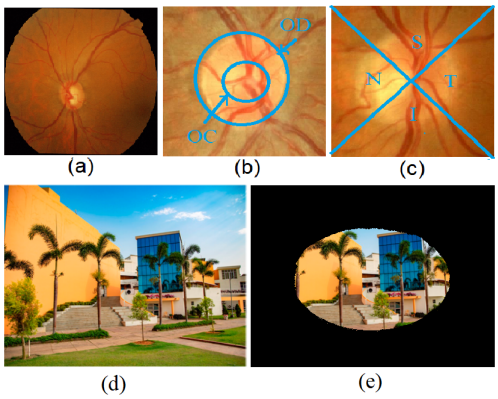

Figure 1. Top: (a) Sample of fundus image, (b) OD and OC regions, (c) ISNT quadrants from Mendeley dataset, Bottom: visual fields with (d) normal, (e) glaucoma cases.

2. Literature review

An automatic glaucoma detection model using retinal imaging basically goes through image quality enhancement, segmentation, feature extraction and classification steps. In this section some literatures related to glaucoma detection are discussed and stepwise classified as follows.

2.1. Methods for image quality enhancement

Radim et al. [6] proposed a preprocessing method based on fractral dimensions by selecting retinal nerve fibres (RNF) as a major indicating parameter for glaucoma detection. Regular damage of RNF is analysed using fractal and power spectral features and SVM for classification. This method is tested on 30 fundus images from Eye Clinic of MUDr Kubena in Zlin (Czech Republic) with 74% classification accuracy which is mainly depended on RNF losses. In Pruthi et al. [7], illumination correction and intensity inhomogeneity are used as a preprocessing step and after that blood vessels, and noises are removed. In feature extraction techniques, the OD and OC regions are segmented and the classification is based on the calculation of CDR. This approach used a batch of 20 images from Vitro Retina Unit, AIIMS, New Delhi, India and Scotland, UK for model implementation and it fails for the images having other pathological diseases. To enhance the quality of each RGB channel individually, Zhou et al. [8] introduced a luminosity adjusting approach by constructing a luminance matrix. This matrix is created by the gamma correction of the values of fundus image channels in HSV colour space. This approach used 1200 retinal images from MESSIDOR

dataset and 961 images from Top Con Medical Systems Tokyo, Japan at the eye centre of second affiliated Hospital of Zhejiang University. The contrast limited adaptive histogram equalisation (CLAHE) technique, which normalizes the histogram of image pixels through an iterative kernel-based process to prevent pixel congestion in a specific range, was used to improve the contrast of images. By maximising the contextual area, Aurangzeb et al. [9] aimed to create some ML models for retina vascular segmentation. After modifying the CLAHE settings with MPSO, traditional assessment methods are used to analyse the performance of the system. The author demonstrated CLAHE's impact on deep learning models for retinal image segmentation utilizing contrast-enhanced images created using MPSO-based on CLAHE from DRIVE and STARE datasets. To improve retinal images Wang et al. [10] used the methods of image decomposition and visual adaptation. Base, detail, and noise layers were separated from the input images and these layers were subsequently subjected to several processing steps, including denoising, detail improvement, and lighting correction. The weight fusion function was used in this model to enhance and denoise images from DIARETDB0 and DIARETDB1 datasets. This technique is utilised a standard visual adaptation model to adjust for uneven illumination.

2.2. Methods for OD and OC segmentation

Geeta et al. [11] developed an enhanced methodology in relation to their earlier research for the localization and segmentation of retinal fundus images in optic discs. For enhancing segmentation, the model used super pixels of the red channel and selected circular Hough peak values. For localization, they used a method of calculation through pixel density to detect disease in fundus images. The method was tested on 8 datasets. When compared to current localization and segmentation approaches, this technique produced better results. The segmentation accuracy of the suggested approach is 99.5%, while the localization accuracy of the optic discs is 99.93%. The Glow worm Swarm Optimization algorithm, a technique for automatic the detection of optic cups from retinal fundus image, was introduced by Pruthi et al. [12]. Although the framework is reliable for glaucoma detection, it cannot calculate the cup-to-disc ratio. Mask-RCNN is a technique that Nazir et al. [13] introduced a clustering method to segment OD and OC lesions. In order to extract the key features and segment the important regions from the fundus images this approach used Mask-RCNN architecture and DenseNet-77 as a backbone. The glaucoma segmentation approach performed well, although segmentation results still require upgrading. One of our previous works [14] that proposed for OD segmentation using robust PCA and using this method, glaucoma detection has been done successfully with four classifiers.

2.3. Methods for feature extraction

50 fundus images were categorised into glaucoma and non-glaucoma classes in a research by Virk et al. [15]. In this study, Virk et al. reached the conclusion that fundus images having CDR values within 0.3 and 0.5 should be labelled as non-glaucomatous and those with values over 0.5 as glaucomatous. While using these threshold values to identify glaucoma, Virk et al. reported an accuracy of 80%. An automated methodology for detecting defects in the retinal nerve fibre layer was proposed by Rashmi Panda et al. [16], since; fundus images provide strong indications of the condition of glaucoma. Loss of vision can be stopped with early detection and prevention. The technique used a patch characteristic-driven RNN to detect objects in fundus images. A dataset of fundus images from the Glaucoma Diagnostic Services, L.V. Prasad Eye Institute, Bhubaneswar, India. is used to monitor performance. High RNFLD detection and precise boundary localization are achieved by this approach. The optic disc was found using eclipse fitting in Ruengkitpinyo et al. [17] and the rim width was calculated using the INST Rule. The obtained key features such as CDR and rim width are used to classify images by support vector machine.

2.4. Methods for Classification

In order to retrieve the OD and OC regions, Karkuzhali et al. [18] used super pixel segmentation to calculate CDR, ISNT, optic nerve head, and the area of the blood vessels are measured. The neural networks with 100% accuracy were trained using 26 images. However, verifying on a limited number of images affected their results. To improve performance, characteristics retrieved by various CNNs were integrated by Li et al. [19] However, these CNN approaches tends to treat all image regions equally rather than giving special consideration to certain regions and reducing noise levels outside of the optic disc area. Li et al. [20] used attention methods to diagnose glaucoma, but the cost and annotator bias of the required human annotated ground truth of attention masks make it impractical. A deep CNN is used by Chen et al. [21] to create ALADDIN, an automated feature learning system for glaucoma detection. The experiments used the ORIGA and SCES datasets, and researchers reported an AUC of 83.8% (ORIGA) and 89.8% (SCES).

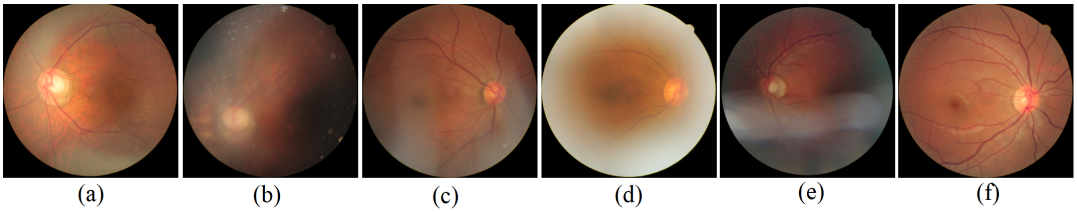

Figure 2. Fundus image instances. (a,b,c,d,e) low quality specular reflected images due to non-uniform illumination (f) High quality image

3. Research gap, motivation, and objectives of research

In biomedical applications, retinal imaging always suffers from non-uniform illumination problem. Due to this, the captured fundus images have low contrast, blurriness, and specular reflection problems which hindrances to diagnose retinal diseases efficiently. From the discussed literatures, it is cleared that many researches have been addressed the first two problems [6-10], but a few for the third problem. The specular reflections are mainly caused by variations in the intensity of illumination, disturbance in the location of the light source and the fundus camera. So, reducing the specularity issue is a pertinent and significant challenge. Figure 2 shows some samples of fundus images having specularity problem and also comparison between high quality and low quality images.

The above observation motivates to use various specular reflection separation algorithms in case of corrupted retinal fundus images. One of the methods, Akashi et al. [26] is based on sparse non-negative matrix factorization (NMF). NMF is one of the popular matrix analytics methods for multivariate data that contains non-negative values like image matrices. NMF has a wide range of applications and can generate recurring patterns. This approach can calculate both the single-color areas and distinct reflection components. Another method proposed by Shen et al. [22] i.e. modified specular free (MSF) to demonstrate some robustness to noise. Tan et al. [25] suggested single image reflection component separation approach with the adjustment of the maximum chromaticity of each pixel to an arbitrary scalar value. The maximum diffuse chromaticity method is used by Yang et al. [27] to separate the specular reflections from an image. This method used a bilateral filter to calculate the diffuse chromaticity, and the coefficients were based on an approximation of the maximum diffuse chromaticity.

The objective of this research is to separate the specular and diffuse reflection components from the corrupted fundus images using modified dichromatic reflection methods and then to apply the obtained high quality image which is free from specular reflections to diagnose glaucoma using segmentation, feature extraction and image classification steps.

The distinctive contributions in this research are as follows.

- The development of preprocessing step for separation of reflection components from the input fundus image using high emphasis filter and similarity function based method. Seven reflection component separation methods are compared and finally the best method is chosen.
- The implementation of modified U-net model for OD and OC segmentation using the specular free fundus image obtained in the first step.
- The extraction of important features such as CDR, NRR, INST to be used as diagnostic parameters in glaucoma detection.
- The detection of glaucomatous images as normal or abnormal, using SVM with different kernels.

The whole paper is organized as follows. Section I provides a summarized introduction of the research. Some existing works that have been done for enhancement of fundus image quality and glaucoma detection models are described in section II. Section III provides a brief discussion about the research problem, objectives, motivation and main contribution of this research. The proposed methodology is described in details in section IV. In section V, the results of the proposed method with discussion and analysis on this result are described. Section VI describes about the conclusion with the contribution and future works.

4. Proposed methodology

The main aim of this proposed method is to achieve the research objectives for automatic glaucoma detection using retinal fundus images. The block diagram of proposed model is shown in figure 3. It consists of a preprocessing step in which seven methods are compared such as Non-negative matrix factorisation method [26], chromaticity based method [22], Modified chromaticity based method [23], intensity ratio based method [24], texture based logarithmic differentiation

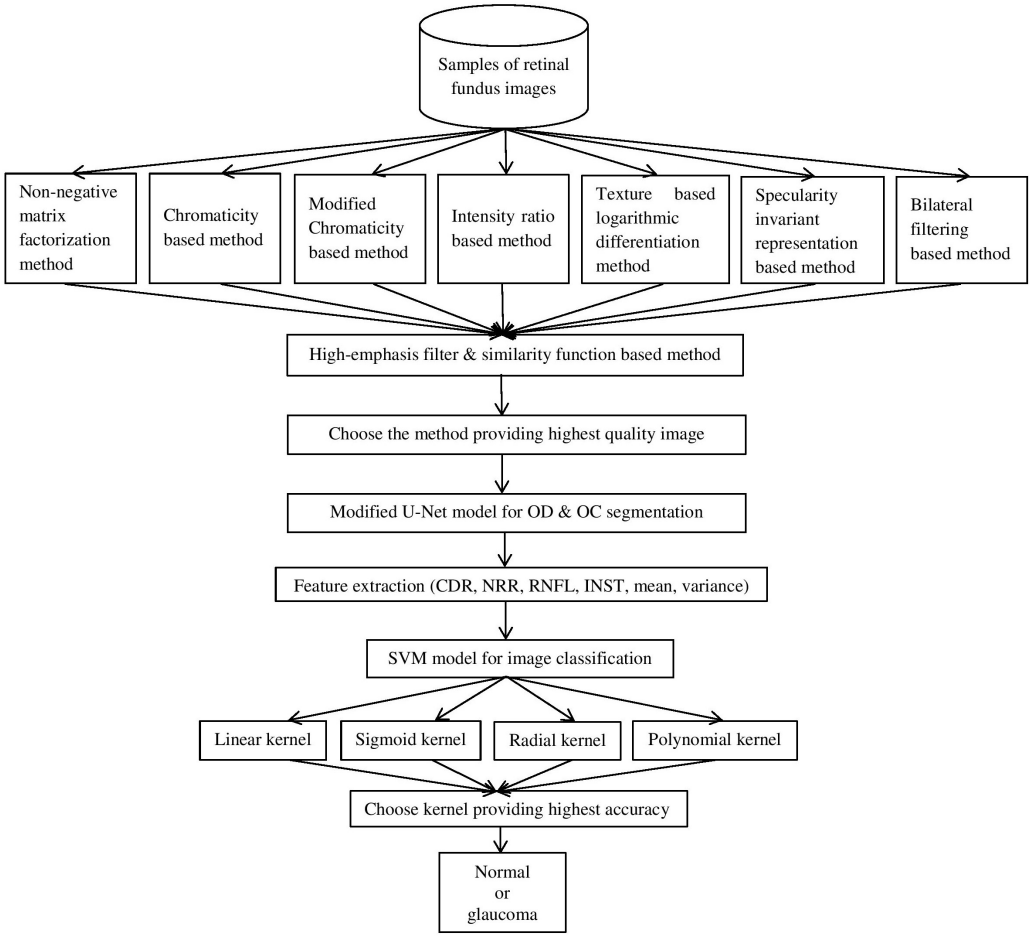

Figure 3. Block diagram of the proposed hybrid model for reflection problem reduction and efficient glaucoma detection

method [25], specularity invariant representation based method [28], and bilateral filtering based method [27] for separating the diffuse and specular components from the input image. Then, high emphasis filter and similarity function based method [30] is applied to both the specular and diffuse components. By choosing the most efficient method among them which provides a specular free fundus image, the next is applied as a segmentation step. In segmentation step, a modified U-net CNN model is used to segment both OD and OC from the specular free fundus image. Then, the next step called feature extraction which extracts the most important features from the segmented OD and OC. In the next step the extracted features are provided as an input to the SVM classifier with different kernels such as linear, sigmoid, radial, and polynomial and by choosing the kernel which provides highest accuracy, the normal or glaucoma classification has been done successfully.

The proposed model is called a hybrid model, because it is a combination of reflection component separation based image processing method, Deep Learning based OD and OC segmentation method, and Machine Learning based image classification method. In this section, the whole framework is divided into two parts such as theoretical and experimental.

4.1. Theoretical framework

Separation of reflection components. As reported by dichromatic reflection model [5], light splits into two components after falling into the surface of an object, which depends upon refractive index of the material. One component is known as the specular reflection, which reflects on the surface in a mirror-like structure and another is the diffuse reflection, which enters the object and disperses before emerging and reflecting. The process of retinal imaging with fundus cameras follow the above dichromatic scattering method and the fundus image captured can be described as:

$$F_c = \alpha_d F_d + \beta_s F_s \tag{1}$$

where F_c is the corrupted fundus image, F_d and F_s are the diffuse and specular fundus images with coefficients of α_d and β_s respectively.

Many methods have been developed by using the dichromatic reflection model for single image highlight removal [22-28]. To reduce the specularity in real world images the authors [29] extended the method of separation based on chromaticity. Yamamoto et al. [30] method used some existing methods for calculating the diffuse reflection component between input image and the image filtered by a high emphasis filter. The step includes in this method are:

- Step 1: Separate the diffuse $(\alpha_d F_d)$ and specular $(\beta_s F_s)$ reflection components from the input image using the existing methods of [22-28].
- Step 2: Apply high emphasis filter on each components separated in step 1 and also on the input image.
- Step 3: Combine the filtered reflection components $(\alpha_d F_d)_h$ and $(\beta_s F_s)_h$, and find the diffused reflection component having error between filtered diffuse component and filtered input image $(F_c)_h$. The criteria for erroneous diffuse component mathematically expressed as follows.

  $(\alpha_d F_d)_h > (F_c)_h$, or $(\alpha_d F_d)_h < 0$
- Step 4: Calculate plausible diffuse reflection component to minimize similarity function (ϕ) with erroneous pixel coordinate (e) and plausible pixel coordinate (p) using input (F_c) , filtered input $((F_c)_h)$ and combined filtered image (F_h).

$$\begin{aligned}\phi(e,p) &= \phi_{input}(e,p) + \phi_{filtered}(p) \\ &= \omega\|F_c(e) - F_c(p)\|_2^2 \\ &+(1-\omega)\|(F_c)_h(p) - F_h(p)\|_2^2\end{aligned} \tag{2}$$

  Where $\phi_{input}(e,p)$ is the input pixel value differences between the coordinates of e and p which is equal to $\omega\|F_c(e) - F_c(p)\|_2^2$. $\phi_{filtered}(p)$ is the high emphasis filtered pixel value differences at coordinate p, which is equal to $(1-\omega)\|(F_c)_h(p) - F_h(p)\|_2^2$ and ω is the weight coefficient.
- Step 5: Replace the diffused error component with plausible diffuse component and check the convergence by using the improved diffuse reflection component $(\alpha_d F_d)'$ as the output of the step 1. The iteration goes on until, it satisfies the following condition.

$$RMSE_{(n,n-1)} < \epsilon \tag{3}$$

where RMSE = Root Mean Square Error between n and n-1, and ϵ is a predetermined threshold value.

Modified U-net CNN. U-Net was presented as a fully convolutional neural network with the ability to train on very minimal datasets and provide results which can be compared with sliding window based models [31]. It performs better than existing approaches on a variety of biomedical image segmentation problems after being trained with particular data augmentation and improvement strategies. In our application, segmentation of OD and OC provides an efficient step for extracting most important features like CDR, which a major indicator of glaucoma screening. Artem Sevastopolsky [32] presented an effective modified U-net model for this OD and OC segmentation. The network has a contracting path and an expansive path, just like the original U-Net. Contracting path architecturally is a pretrained model of convolution such as the VGG-16. On the expansive path, data from layers of the contracting path with the proper resolution and layers of the expansive path with lower resolution are combined, allowing the entire network to recognise patterns at various scales. The input image is initially processed through a convolutional layer with less number of filters with a spatial resolution of 3×3 pixels. The Dropout regularisation and ReLu activation function are then used (f(x) = max (0, x)). The same is done repeatedly, and the Max Pooling technique is used to halves the image's width and height. After that, the image is processed through the aforementioned layer sequence until the low resolution. The same CNN layers are used on the expanding path, mixed in with upsampling layers that trivially increase image width and height by two. It is important to note that the revised U-net model can segment OD and OC on a fundus image, therefore there is no requirement of any preparatory cropping of input images to area of the OD.

Retinal image features. The extraction of features is established when the segmentation process is completed. In this research, several features are derived from the segmented images. These characteristics lead to better glaucoma detection outcomes. The features utilised for classification include the Cup-to-Disc Ratio (CDR), Retinal nerve fibre layer (RNFL), Neuro-Retinal Rim (NRR), Haralick features, etc.

- Cup to Disc Ratio (CDR) : It is the ratio between area of OC and area of OD. The CDR value for a typical disc is less than 0.5, whereas the CDR value for a glaucoma affected image is greater than 0.5.

$$CDR = \frac{Area\ of\ Optic\ Cup\ (OC)}{Area\ of\ Optic\ Disc\ (OD)} \tag{4}$$

- Neuro-retinal rim (NRR) : It is referred to as the space between the edges of the optic disc and the

optic cup. Because of the regions in nasal develop thicker than other areas in temporal, a part of the area is demonstrated as NRR, and the NRR is active in both inferior and superior regions. The area of NRR is provided by the AND operation between the optical disc and optical cup.

- INST features : For the purpose of optic disc image segmentation, the INST features shows the ratio of the blood vessel area present in the superior and inferior to the temporal and nasal regions.
- Retinal nerve fibre layer (RNFL) : The expansion of the optic nerve fibres having thickest layer close to the OD creates RNFL. It is typically seen in the inferior temporal region of the normal eye, followed by the S-T regions, I-N, and T-N.
- Statistical features : This statistical feature extraction describes a number of features including mean, variance, and others. To calculate the average number of white pixels, use the term mean. The information about the image contrast is separated by variance, which is dependent on the mean value.

SVM classifier. The support vector machine (SVM) is a precise classification algorithm that divides the input datasets into two categories. The margin-maximizing line that separates the two classes is represented by the support vector. The kernel SVM can be enhanced with additional features to match a hyper plane and making it appropriate for nonlinear data. The SVM model in this instance uses four kernels: linear, sigmoid, RBF, and polynomial. The best among the four is identified to diagnose glaucoma. The following steps were taken in order to develop the SVM model:

- Step 1: Separation of the whole dataset into training and test data.
- Step 2: Usage of the support vector based principle to simulate the model.
- Step 3: Implementation of kernel functions.
- Step 4: Prediction of diseases classes using the proposed model on test data.
- Step 5: Calculation of performance matrices from the testing results.

4.2. Experimental framework

Data resources. A total of 2,206 anonymous retinal images constitutes the Mendeley data repository [39]. It includes both healthy and abnormal retinal images collected from different datasets. MESSIDOR, HRF, FIRE, DRIVE, Kaggle DMR, and publicly accessible images from Google image search might all be included in this dataset. To study artefact reduction, images with and without artefacts were grouped. Finally, 1146 artefact-containing images and 1,060 artefact free images were grouped. The declaration of Helsinki was followed throughout the experimental process. For experimentation the images are split into training (80%) and testing data (20%).

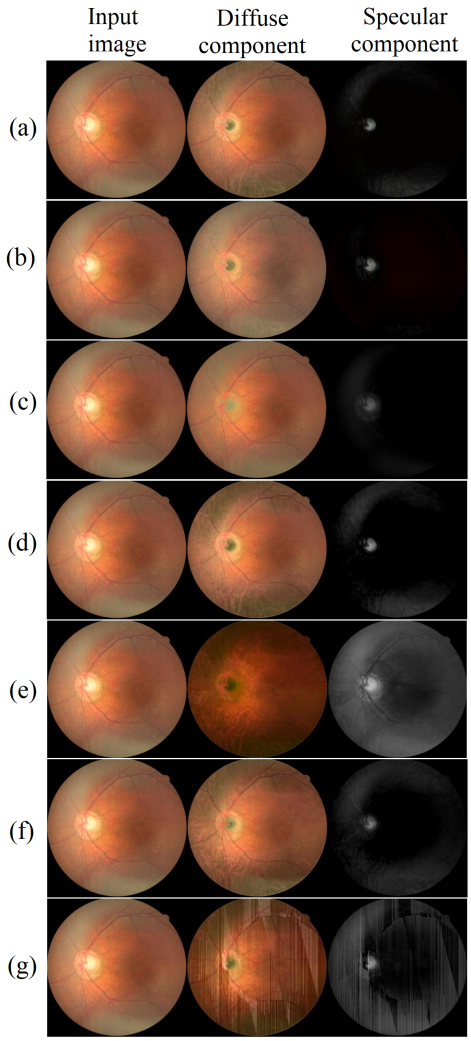

Figure 4. Separated diffuse and specular fundus images using seven existing methods, (a) Akashi et al. [26], (b) Shen et al. [22], (c) Shen et al. [23], (d) Shen et al. [24], (e) Tan et al. [25], (f) Yang et al. [27], (g) Yoon et al. [28]

Parameter settings. The experiments are conducted using retinal fundus images having specular reflections from the discussed dataset to test the effectiveness of the proposed method by using some static parameters and applied conditions. The weight coefficient ω is taken as 0.3 in the similarity function, convergence parameter ϵ is set as 0.2 with 10 iterations for all experiments.

Table 1. Performance comparision of PSNR and SSIM values among seven methods with improved methd [29]

Methods	PSNR	Improved PSNR	SSIM	Improved SSIM
Akashi et al. [26]	28.15	29.52	0.893	0.892
Shen et al. [22]	26.32	26.85	0.882	0.893
Shen et al. [23]	32.43	32.91	0.935	0.941
Shen et al. [24]	35.32	37.97	0.952	0.961
Tan et al. [25]	26.32	26.81	0.873	0.872
Yang et al. [27]	29.25	30.78	0.892	0.881
Yoon et al. [28]	23.42	24.78	0.621	0.632
Average	28.74	29.94	0.864	0.867

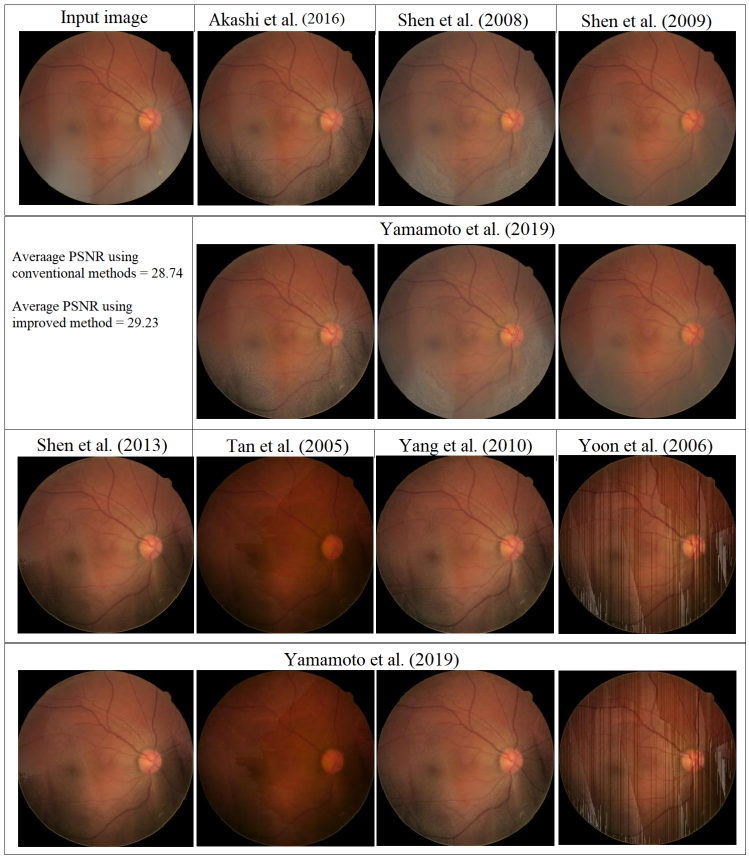

Figure 5. Improvement in diffused images after using seven methods with Ymamamoto et al. [30]

Model implementation. All experimentation works were conducted on a PC with Intel (R) Core (TM) i7 - 3770 CPU and 8:00 GB RAM. The preprocessing algorithms for separating the diffuse and specular components were implemented in MATLAB R2019a without any GPU acceleration. The algorithms for OD and OC segmentation and image classification were implemented using the Google CoLaboratory, a free cloud service for sharing deep learning research which offers a programming environment with powerful graphics processing (GPU) and deep learning libraries based on Tensorflow. This makes it possible to run a powerful deep learning network quickly without a personal GPU. A Google Drive account's fundus image dataset was put into the CoLaboratory's environment.

In this model the input images having refection problem depicted in Fig 2 are taken as input to the seven discussed methods for separating diffuse and specular components. First, we use the discussed methods to get diffuse and specular components. There is a comparison between seven methods which provided the most appropriate reflection components separation. Then, for each component, a high-emphasis filter is applied. We can identify erroneous pixels because the high-emphasis filter responses on the failed region grow more as compared to original. As a result, we take into

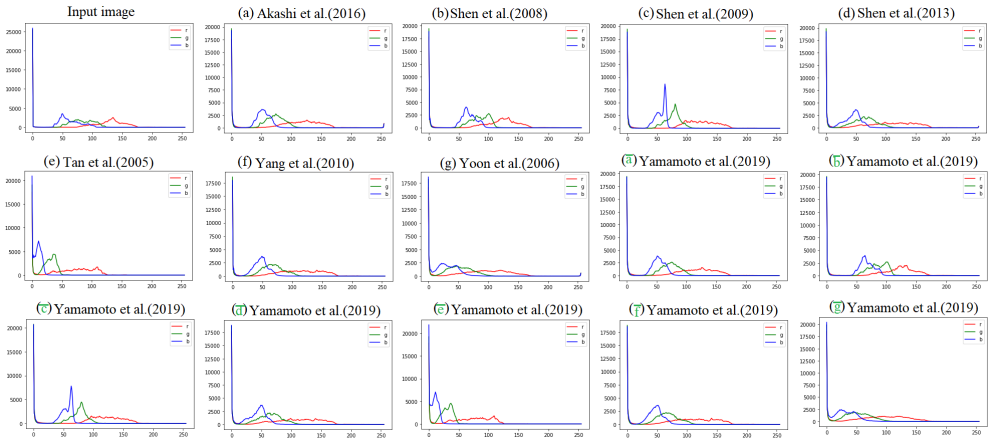

Figure 6. Histogram of input and specular free images showing effect of specularity in R, G and, B channels.

account the similarity between the target and reference pixels and substitute the results of these erroneous pixels with those of other reference pixels from the image.

The specular free diffuse images from the most appropriate method are taken as a input to the modified U-Net segmentation model. This model is applied on both OD and OC segmentation to extract the retinal image features. The most important features discussed in the previous section are extracted and used for normal or abnormal image classification using SVM. The classification experiment is conducted by comparing four discussed kernels of SVM and the best kernel is chosen for classification.

5. Results and discussion

The convenience of the results obtained from the preprocessing step is checked by Peak Signal-to-Noise Ratio (PSNR) and Structural Similarity Index (SSIM) values. By using both the conventional and improved approaches in the image enhancement step the results are summarized in table 1. Peak error is represented as PSNR (in dB). The visual and structural information retained in the output image is measured using SSIM. The SSIM index measure ranges from 0 to 1, with 1 denoting comparable images and 0 denoting structurally fully uncorrelated images. The PSNR from the seven methods are shown in the first column of table I. Shen at al. [25] shows a maximum PSNR value of 35.32 dB which further improved by using Yamamoto et al. [30] in the second column of that table showing as improved PSNR is 37.97dB. Similarly, the SSIM using Shen at al. [25] method shows maximum value of 0.952 and improved value of 0.961 using Yamamoto et al. [30].

The comparison between the output images of seven conventional methods and the improved methods are shown in figure 5. These experimental findings demonstrate that, in comparison to conventional

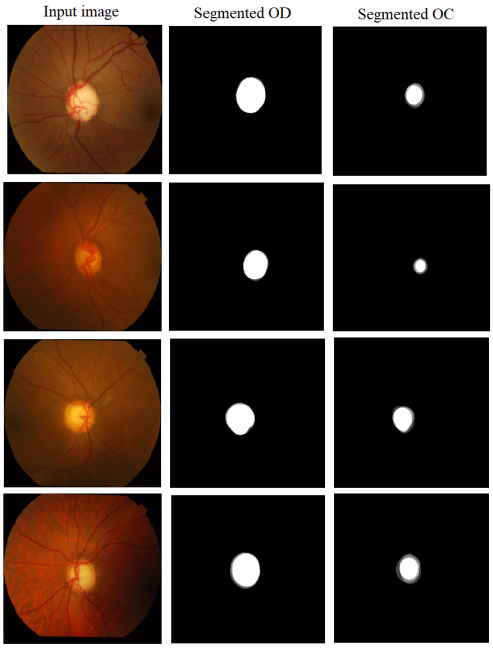

Figure 7. Sample of input images with segmented OD and OC images.

methods, the improved strategy increases the accuracy of reflection separation in all the corrupted fundus images with respect to PSNR values. With the help of the similarity function, this method increases the accuracy of reflection separation while employing the computed diffused component. As a result, the improvement in dB is dependent on how accurately the predicted diffuse reflection component is separated. The output diffuse and specular components separated from the input image using seven conventional methods are shown in figure 4. The improved method eliminates artefacts as black and white pixels in the diffuse and specular components, and around colour boundaries as

Table 2. Performance comparision of proposed hybrid model with existing glaucoma detection methods

Author	Year	Technique	Dataset	Performance
Serte et al.[33]	2020	Ensemble of CNN	HARVARD	SEN: 86%, Acc: 88%, SPEC:90%, AUC:0.94
Pathan et al.[34]	2021	ANN, SVM	DRISTI-GS1, Private from Kasturba Medical College (KMC)	SEN: 93.47%, Acc: 90% SPEC:91.21%
Bao et al.[35]	2021	self-adaptive transfer learning (SATL)	LAG, private, REFUGE-2	SEN: 71.38%, Acc: 74% PRE:59.55%
Chaudhary et al.[36]	2021	2D-FBSE-EWT	RIM-ONE-r1, RIM-ONE-r2, RIM-ONE-r3, ORIGA, DRISHTI-GS1	SEN: 94%, Acc: 91%, SPEC:83%, AUC:0.96
Huang et al.[37]	2022	Fine grained grading deep learning (FGG-DL)	Humphery, Octopus visual fields	Acc: 85%, 90%, AUC: 0.93, 0.9
R. Fan et al.[38]	2022	Data efficient image Transformer (DeiT)	OHTS	AUC: 0.87, 0.93
Proposed hybrid model	-	Reflection components separation, modified U-Net, SVM	Mendeley Data repositories	Acc: 91.83%, SEN: 96.39%, SPEC: 95.37%, AUROC: 0.972

compared to the outcomes of conventional methods. In comparison to Tan et al. method, the improved method decreases white colour artefacts produced by insufficient specular removal. This method minimizes artefacts produced by excessive specularity removing around the disc boundary, which are presented as magnified images in comparison to the outcome of Yang et al. method. This method does not significantly improve the computed diffuse component from Shen et al. method with less number of high frequency components. Erroneous diffuse pixels are found using our approach, which employs the high emphasis filter. Figure 6 shows the histogram of the input image having specularity problem and the output specular free images. Figure 6(a) to 6(g) are the histogram of output images using seven methods [22-28]. The difference of intensity values among seven plots in figure 6(a) to 6(g) are compared with the input specular image. After removal of specularities the intensity value increases and the maximum smoothness is shown in figure 6(d) using Shen et al. [24]. Then, by taking all seven output images as a input to Yamamoto et al. [30] method and high emphasis filtering, the histograms are shown in the last seven plots of figure 6. The lowest intensity shown in red channel with right shifting, green chanel shows medium intensity and blue has high intensity.

In the segmentation experiment, the improved approach based on modified U-Net can produce results equivalent to or better than already existing. The same approach, used for both OD and OC segmentation, produces high-quality results, demonstrating its suitability for use with other image recognition issues. The segmented OD and OC binary images are shown

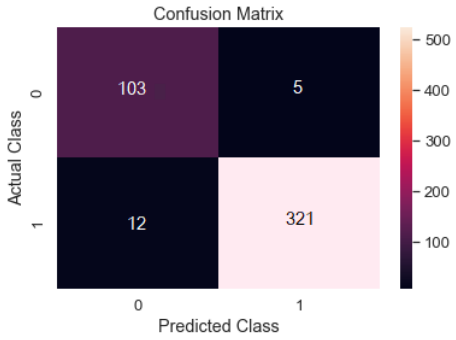

Figure 8. Confusion matrix obtained after classification showing true positive (TP), true negative (TN), false positive (FP) and false negative (FN)

in figure 7. The simplicity with straightforward modern frameworks and shortest prediction time of the proposed approach are further benefits. Results from experiments and visual comparisons demonstrate that automatic OD segmentation can be performed at a level of quality comparable to that of a manual segmentation. Optic cup, on the other hand, is more difficult to identify, which is reinforced by the fact that its border is considerably more delicate. The extracted features from the segmented images are feed to the SVM classifier with four numbers of kernels. By choosing the kernel which provides highest accuracy, the confusion matrix obtained shown in figure 8. From the confusion matrix, the performance indices are calculated using the following formulas. The calculated Accuracy, sensitivity and specificity are 91.83%, 96.39%, and 95.37% respectively.

$Accuracy = \frac{TP+TN}{TP+TN+FP+FN}$, $Sensitivity = \frac{TP}{TP+FN}$

$Specificity = \frac{TN}{TN+FP}$

The proposed approach is compared with some recent updated models shown in the table 2. Chaudhary et al. [36] proposed a 2D-FBSE-EWT method to decompose the input image and these images were used for glaucoma detection with an accuracy of 91%. Bao et al. [35] presented a self-adaptive transfer learning (SATL) method to enhance the classification performance of a target domain and showed 74% accuracy. Pathan et al. [34] used ANN and SVM classifier for preprocessing, segmentation and classification of images with an accuracy of 90%. Serte et al. [33] proposed an ensemble CNN model for accurate detection of glaucoma and show 88% accuracy. In figure 9 the ROC curve of proposed hybrid model is compared with four recent methods. Our method outperforms an area under the ROC of 0.971 as compared to other methods.

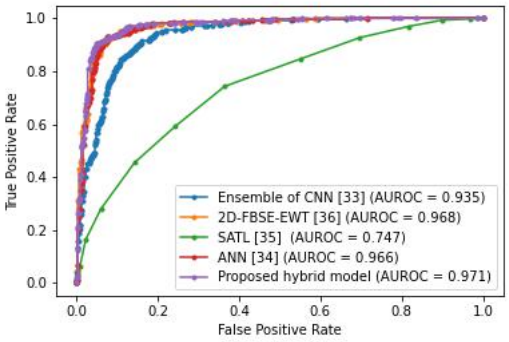

Figure 9. ROC of proposed hybrid model compared with some existing methods with the area.

6. Conclusion

In this research, we propose a hybrid glaucoma detection model which is a combination of conventional image processing, machine learning and deep learning methods. Our aim is to remove specularity from retinal fundus images which prone to an efficient screening of glaucoma. We implemented a modified method of dichromatic reflection model for diffuse and specular components separation. We employed a non-linear high emphasis filter and calculate a similarity function for separating the reflection components efficiently. Particularly, in high frequency regions where traditional approaches fail to accurately remove the specular components; our method could produce better separation results. We have extended this specularity removal method to predict glaucoma and for that we used modified U-net for segmentation, feature extraction, and SVM for classification. The experimental analysis proved that by using this specularity removal method the accuracy, sensitivity and specificity is increased as compared to other existing methods. However, the future study will extend this hybrid model to other biomedical images and also for diseases detection problem.

References

[1] M. D. Abramoff, M. K. Garvin, and M. Sonka, Retinal imaging and image analysis, IEEE reviews in biomedical engineering, vol. 3, pp.169-208, 2010.

[2] H. Wang, S. Lin, X. Liu, and S. B. Kang, Separating reflections in human iris images for illumination estimation, in Tenth IEEEInternational Conference on Computer Vision (ICCV05) Volume 1,vol. 2. IEEE, 2005, pp. 1691-1698.

[3] D. Bhowmik, K. S. Kumar, L. Deb, S. Paswan, and A. Dutta, Glaucoma-a eye disorder its causes, risk factor, prevention and medication. The Pharma Innovation, vol. 1, no. 1, Part A, p. 66, 2012.

[4] R. Shinde, Glaucoma detection in retinal fundus images using u-net and supervised machine learning algorithms, Intelligence-Based Medicine,vol. 5, p. 100038, 2021.

[5] S. A. Shafer, Using color to separate reflection components, Color Research and Application, vol. 10, no. 4, pp. 210-218, 1985.

[6] R. Kola r and J. Jan, Detection of glaucomatous eye via color fundusimages using fractal dimensions, Radioengineering, vol. 17, no. 3, pp.109-114, 2008.

[7] J. Pruthi and S. Mukherjee, Computer based early diagnosis of glaucoma in biomedical data using image processing and automated earlynerve fiber layer defects detection using feature extraction in retinalcolored stereo fundus images, International Journal of Scientific and Engineering Research, vol. 4, no. 4, p. 1822, 2013.

[8] M. Zhou, K. Jin, S. Wang, J. Ye, and D. Qian, Color retinal image enhancement based on luminosity and contrast adjustment, IEEE Transactions on Biomedical engineering, vol. 65, no. 3, pp. 521-527, 2017.

[9] K. Aurangzeb, S. Aslam, M. Alhussein, R. A. Naqvi, M. Arsalan, and S. I. Haider, Contrast enhancement of fundus images by employing modified pso for improving the performance of deep learning models, IEEE Access, vol. 9, pp. 47 930-47 945, 2021.

[10] J. Wang, Y.-J. Li, and K.-F. Yang, Retinal fundus image enhancement with image decomposition and visual adaptation, Computers in Biologyand Medicine, vol. 128, p. 104116, 2021.

[11] R. G. Ramani and J. J. Shanthamalar, Improved image processing techniques for optic disc segmentation in retinal fundus images, BiomedicalSignal Processing and Control, vol. 58, p. 101832, 2020.

[12] J. Pruthi, K. Khanna, and S. Arora, Optic cup segmentation from retinal fundus images using glowworm swarm optimization for glaucoma detection, Biomedical Signal Processing and Control, vol. 60, p. 102004,2020.

[13] T. Nazir, A. Irtaza, and V. Starovoitov, Optic disc and optic cup segmentation for glaucoma detection from blur retinal images usingimproved mask-rcnn, International Journal of Optics, vol. 2021, 2021.

[14] Lenka, S., and Lazarus, M. Z. (2022, December). Optic Disc Segmentation using Nonconvex Rank Approximation from Retinal Fundus Images. In 2022 IEEE 2nd International Symposium on Sustainable Energy, Signal Processing and Cyber Security (iSSSC) (pp. 1-6). IEEE.

[15] J. K. Virk, M. Singh, and M. Singh, Cup-to-disk ratio (cdr) determination for glaucoma screening, in 2015 1st International Conference onNext Generation Computing Technologies (NGCT). IEEE, 2015, pp.504-507.

[16] R. Panda, N. B. Puhan, A. Rao, D. Padhy, and G. Panda, Recurrent neural network based retinal nerve fiber layer defect detection in earlyglaucoma, in 2017 IEEE 14th International Symposium on BiomedicalImaging (ISBI 2017). IEEE, 2017, pp. 692-695.

[17] W. Ruengkitpinyo, P. Vejjanugraha, W. Kongprawechnon, T. Kondo, P. Bunnun, and H. Kaneko, An automatic glaucoma screening algorithm using cup-to-disc ratio and isnt rule with support vector machine, in IECON 2015-41st Annual Conference of the IEEE Industrial ElectronicsSociety. IEEE, 2015, pp. 000 517-000 521.

[18] S. Karkuzhali and D. Manimegalai, Computational intelligencebased decision support system for glaucoma detection, BIOMEDICALRESEARCH-INDIA, vol. 28, no. 11, pp. 4737-4748, 2017.

[19] A. Li, Y. Wang, J. Cheng, and J. Liu, Combining multiple deep features for glaucoma classification, in 2018 IEEE International Conference onAcoustics, Speech and Signal Processing (ICASSP). IEEE, 2018, pp.985-989.

[20] L. Li, M. Xu, X. Wang, L. Jiang, and H. Liu, Attention based glaucoma detection: a large-scale database and cnn model, in Proceedings of theIEEE/CVF conference on computer vision and pattern recognition, 2019,pp. 10 571-10 580.

[21] X. Chen, Y. Xu, S. Yan, D. W. K. Wong, T. Y. Wong, and J. Liu, Automatic feature learning for glaucoma detection based on deeplearning, in International conference on medical image computing andcomputer-assisted intervention. Springer, 2015, pp. 669-677.

[22] H.-L. Shen, H.-G. Zhang, S.-J. Shao, and J. H. Xin, Chromaticity based separation of reflection components in a single image, PatternRecognition, vol. 41, no. 8, pp. 2461-2469, 2008.

[23] H.-L. Shen and Q.-Y. Cai, Simple and efficient method for specularity removal in an image, Applied optics, vol. 48, no. 14, pp. 2711-2719,2009.

[24] H.-L. Shen and Z.-H. Zheng, Real-time highlight removal using intensity ratio, Applied optics, vol. 52, no. 19, pp. 4483-4493, 2013.

[25] K. Ikeuchi, D. Miyazaki, R. T. Tan, and K. Ikeuchi, Separating reflection components of textured surfaces using a single image, DigitallyArchiving Cultural Objects, pp. 353-384, 2008.

[26] Y. Akashi and T. Okatani, Separation of reflection components by sparse non-negative matrix factorization, in Computer Vision-ACCV2014: 12th Asian Conference on Computer Vision, Singapore, Singapore,November 1-5, 2014, Revised Selected Papers, Part V 12. Springer,2015, pp. 611-625.

[27] Q. Yang, S. Wang, and N. Ahuja, Real-time specular highlight removal using bilateral filtering, in European conference on computer vision.Springer, 2010, pp. 87-100.

[28] K.-J. Yoon, Y. Choi, and I. S. Kweon, Fast separation of reflection components using a specularity-invariant image representation, in 2006international conference on image processing. IEEE, 2006, pp. 973-976.

[29] Thomas, N., Zefree Lazarus, M., and Gupta, S. (2020). Separation of Diffuse and Specular Reflection Components from Real-World Color Images Captured Under Flash Imaging Conditions. In Energy Systems, Drives and Automations: Proceedings of ESDA 2019 (pp. 265-275). Springer Singapore.

[30] T. Yamamoto and A. Nakazawa, General improvement method of specular component separation using high-emphasis filter and similarityfunction, ITE Transactions on Media Technology and Applications,vol. 7, no. 2, pp. 92-102, 2019.

[31] O. Ronneberger, P. Fischer, and T. Brox, U-net: Convolutional networks for biomedical image segmentation, in Medical Image Computingand Computer-Assisted Intervention-MICCAI 2015: 18th InternationalConference, Munich, Germany, October 5-9, 2015, Proceedings, Part III18. Springer, 2015, pp. 234-241.

[32] A. Sevastopolsky, Optic disc and cup segmentation methods for glaucoma detection with modification of u-net convolutional neuralnetwork, Pattern Recognition and Image Analysis, vol. 27, pp. 618-624, 2017.

[33] S. Serte and A. Serener, Graph-based saliency and ensembles of convolutional neural networks for glaucoma detection, IET ImageProcessing, vol. 15, no. 3, pp. 797-804, 2021.

[34] S. Pathan, P. Kumar, R. M. Pai, and S. V. Bhandary, Automated segmentation and classifcation of retinal features for glaucoma diagnosis, Biomedical Signal Processing and Control, vol. 63, p. 102244, 2021.

[35] Y. Bao, J. Wang, T. Li, L. Wang, J. Xu, J. Ye, and D. Qian, Selfadaptive transfer learning for multicenter glaucoma classification infundus retina images, in Ophthalmic Medical Image Analysis: 8thInternational Workshop, OMIA 2021, Held in Conjunction with MICCAI 2021, Strasbourg, France, September 27, 2021, Proceedings 8.Springer, 2021, pp. 129-138.

[36] P. K. Chaudhary and R. B. Pachori, Automatic diagnosis of glaucoma using two-dimensional fourier-bessel series expansion based empiricalwavelet transform, Biomedical Signal Processing and Control, vol. 64,p. 102237, 2021.

[37] Huang, Xiaoling, Kai Jin, Jiazhu Zhu, Ying Xue, Ke Si, Chun Zhang, Sukun Meng, Wei Gong, and Juan Ye, A structure-related fine-grained deep learning system with diversity data for universal glaucoma visual field grading, Frontiers in Medicine 9, 2022.

[38] Fan, R., Alipour, K., Bowd, C., Christopher, M., Brye, N., Proudfoot, J.A., Goldbaum, M.H., Belghith, A., Girkin, C.A., Fazio, M.A. and Liebmann, J.M., Detecting Glaucoma from Fundus Photographs Using Deep Learning without Convolutions: Transformer for Improved Generalization. Ophthalmology Science, 3(1), p.100233, 2022.

[39] T. K. Yoo, J. Y. Choi, and H. K. Kim, Cyclegan-based deep learning technique for artifact reduction in fundus photography, Graefe's Archive for Clinical

and Experimental Ophthalmology, vol. 258, no. 8, pp. 1631–1637, 2020. https://data.mendeley.com/datasets/dh2x8v6nf8.